arXiv:hep-ph/9509300v1 14 Sep 1995

SCIPP 95/40
August 1995
hep-ph/9509300

Top Quark Physics at the NLC[1]

Carl R. Schmidt [2]
Santa Cruz Institute for Particle Physics
University of California, Santa Cruz, CA 95064, USA

Abstract

A high energy e^+e^- linear collider (NLC) is an excellent tool for studying the properties of the top quark. In this talk I review some of the theory of top quark production and decay in e^+e^- collisions both at threshold and in the continuum. I also report on the results of phenomenological analyses of $t\bar{t}$ production at the NLC.

[1]Invited talk presented at the Workshop on Physics of the Top Quark, Ames, Iowa, May 25 & 26, 1995

[2]Supported in part by the U.S. Department of Energy.

1 Introduction

A high energy electron-positron collider, which I will generically refer to as the Next Linear Collider or NLC, is an ideal tool for studying the properties of the top quark. The event environment in e^+e^- collisions is clean so that precision measurements are possible. The luminosity, which is expected to be on the order of 50 fb^{-1}/yr, is sufficient to provide a yearly sample of a few times 10^4 top pairs. In addition the high degree of electron polarization attainable at the NLC will be very useful for probing the top quark couplings to the photon and Z boson. Although I will not discuss it here, there is also the possibility for a high-energy photon collider mode using back-scattered lasers, which adds significantly to the versatility of the machine. There have been a number of studies of top quark physics at the NLC[1]. In this talk I will discuss some of the highlights, and I will report on the results of a few selected phenomenological studies.

The CDF and D0 collaborations at Fermilab have obtained mass values for the top quark of $176 \pm 8 \pm 10$ and $199^{+19}_{-21} \pm 22$ GeV, respectively[2]. This large mass indicates that the top quark feels the strongest coupling to the symmetry breaking sector of any of the observed particles. Thus, the top quark interactions are an obvious place to look for hints into the dynamics of symmetry breaking. More prosaically, the large mass has an important impact on top quark phenomenology. For large m_t, the top width grows as

$$\Gamma_t \sim 1.7 \text{ GeV} \left[\frac{m_t}{175 \text{ GeV}}\right]^3 \tag{1}$$

This implies that the time required for a top quark to decay is almost always less

than the time for hadronization to occur. The decay time is also significantly less than the time it takes for a top quark to depolarize. Therefore, to a good approximation, the top quark can be treated as a free quark which transfers its polarization to its decay products with little effect from hadronization.

2 The Top at Threshold

The large top width is important at threshold because one of the quarks will typically decay before the $t\bar{t}$ pair can form a bound state. Thus, unlike the case for $c\bar{c}$ and $b\bar{b}$, the $t\bar{t}$ threshold will not be dominated by large resonances. However, for this very reason, it is possible to perform an accurate calculation of the $t\bar{t}$ threshold cross section in QCD perturbation theory. At the nth order in perturbation theory one finds a correction to the photon-$t\bar{t}$ vertex of order $(\alpha_s/v)^n$, where v is the top quark velocity. The infinite sum of these corrections which diverge as $v \to 0$ can be written as the solution to a Schrödinger Green's function equation

$$\Big[-\frac{\nabla^2}{m_t} + V(\vec{r}) - E\Big] G_E(\vec{r}) \;=\; \delta^3(\vec{r}) \tag{2}$$

with $E = \sqrt{s} - 2m_t$ and with the QCD potential $V(\vec{r}) = -(4/3)\alpha_s/r$ at short distances. The total cross section to $t\bar{t}$ pairs is then given in terms of the Green's function by $\sigma \sim \mathrm{Im} G_E(0)$.

For the bottom and charm quarks, the singularity at small velocities is cured by the QCD confining potential at long distances. For the top, however, Fadin and Khoze[3] showed that it was possible to include the width effects by replacing $E \to E + i\Gamma_t$. The singularity is then cut off by Γ_t with little dependence on

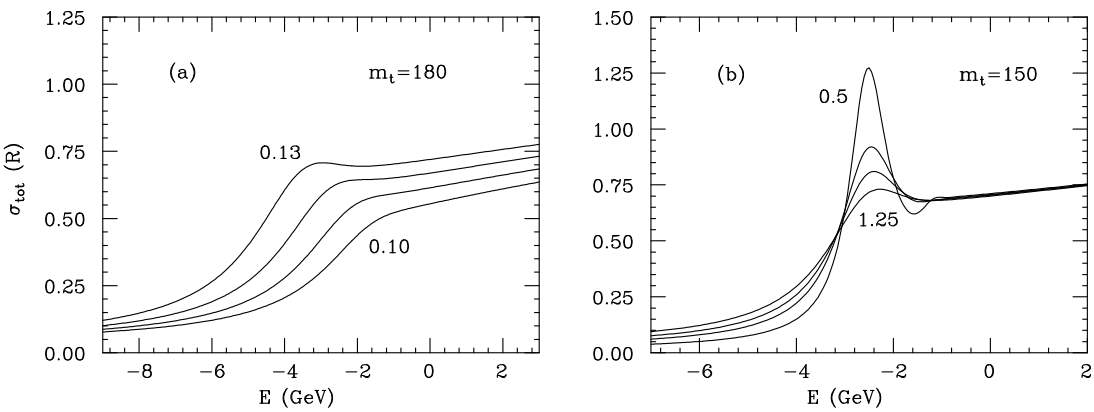

Fig. 1: The $t\bar{t}$ cross section at threshold. The curves in (a) correspond to $\alpha_s = .10$, .11, .12, and .13. The curves in (b) are with α_s fixed to .12 and the top width set to 0.5, 0.8, 1.0, and 1.25 times its Standard Model value.

the long distance potential. The $t\bar{t}$ threshold cross section can be unambiguously computed as a function of α_s, Γ_t, and the top mass m_t.

In Fig. 1(a) I present a plot[4] of the cross section as a function of energy for a top quark of 180 GeV and several different values of α_s. One can see from this plot that the measurements of m_t and α_s are highly correlated; i.e., a change in m_t can be substantially mimicked by a change in α_s. It is still possible, however, to get a very precise value of m_t. In a detailed Monte Carlo analysis using 11 cross section measurements of 1 fb^{-1} each, and assuming a nominal top mass of 170 GeV, Fujii *et al.*[5] were able to extract m_t with an estimated error of 380 GeV with α_s unconstrained. Certainly, the error will be even smaller if α_s is known precisely from an independent experiment.

The effect on the cross section of a nonstandard top quark width is shown

in Fig. 1(b) for a top quark of 150 GeV. Assuming α_s is known exactly, Fujii *et al.* found that the width could be measured with a relative error of 18%. If the standard model Higgs is light enough, it can also affect the cross section by giving an additional contribution to the potential of $\Delta V = (\lambda_t^2/4\pi)(1/r)\exp(-m_H r)$. For Higgs bosons of less than about 100 GeV, Fujii *et al.* found that λ_t should be measurable to about 25%.

Beyond simply measuring total $t\bar{t}$ cross section, one can probe the same parameters with different error correlations by looking at kinematic distributions of the top quark. For example, the top quark momentum distribution can be obtained from the Green's function solution to equation (2) by[6]

$$\frac{d\sigma}{d^3\vec{p}} \sim \left|\tilde{G}_{E+i\Gamma_t}(\vec{p})\right|^2. \tag{3}$$

Similarly, the top quark forward-backward asymmetry at threshold, arising from the interference between the different $t\bar{t}$ angular momentum states will be observable.

3 The Top in Continuum

In continuum $e^+e^- \to t\bar{t}$ production the obvious way to measure m_t is by kinematic reconstruction of the event, in a manner similar to that used at the Tevatron. The advantage of the NLC is that the initial state is colorless, so that the events will be cleaner. However, the treatment of QCD radiation in the final state must still be considered. The possibility of gluons radiating off the top quarks and the bottom quarks, both before and after the top decay, renders this a nontrivial problem. In

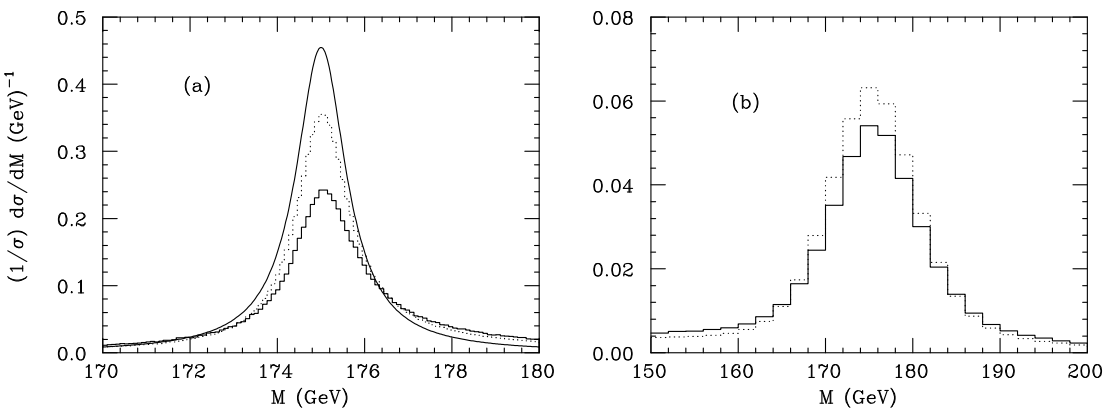

Fig. 2: Top mass reconstruction distributions in the lepton+jets mode without (a) and with (b) detector energy smearing. The dotted histograms are at tree-level, the solid histograms are at $\mathcal{O}(\alpha_s)$, and the smooth curve in (a) is the original Breit-Wigner distribution.

fact, recently there have been reports of discrepancies between $\mathcal{O}(\alpha_s)$ calculations and standard Monte Carlo programs[7].

Although a complete phenomenological analysis of the continuum production is yet to be done, I have performed a simplified analysis at $\mathcal{O}(\alpha_s)$ in the production and the decay of the top quark, using the narrow top-width approximation[8]. Convoluting with a Breit-Wigner line shape for the top quark squared-momentum produces an infrared-finite distribution in perturbative QCD. Fig. 2(a) displays the mass distribution for a 175 GeV top quark in the lepton+jets mode at a 400 GeV center-of-mass collider. The existence of an additional radiated gluon in the production or decay of the top quark can confound the event reconstruction, producing the degradation of the signal at $\mathcal{O}(\alpha_s)$. Note, however, that the peak value of the distribution has not shifted.

In Fig. 2(b) I show the same distribution, but with Gaussian smearing of the final-state lepton and jet energies due to the detector resolution. The smearing parameters used are

$$\frac{\sigma_E^{had}}{E} = \frac{0.4}{\sqrt{E}} , \qquad \frac{\sigma_E^{lep}}{E} = \frac{0.15}{\sqrt{E}} . \tag{4}$$

From this we see that, although QCD radiation effects are certainly non-negligible, the dominant systematic error will probably be due to detector resolution. The mass measurement in continuum is expected to be less accurate than at threshold, but it will definitely be useful due to the different systematic errors involved in the two determinations.

The process $e^+e^- \to t\bar{t}$ in continuum is probably the best place to study the couplings of the top quark to the photon and the weak gauge bosons. Expressed in terms of form factors, the $\gamma, Z \to t\bar{t}$ production vertices are

$$i\mathcal{M}^{i\mu} = ie\Big\{\gamma^\mu[Q_V^i F_{1V}^i + Q_A^i F_{1A}^i \gamma_5] + \frac{i\sigma^{\mu\nu}q_\nu}{2m_t}[Q_V^i F_{2V}^i + Q_A^i F_{2A}^i \gamma_5]\Big\} , \tag{5}$$

where the superscript is $i = \gamma, Z$. In this formula $Q_V^\gamma = Q_A^\gamma = \frac{2}{3}$, $Q_V^Z = (\frac{1}{4} - \frac{2}{3}s^2)/sc$, and $Q_A^Z = (-\frac{1}{4})/sc$, so that at tree level in the standard model $F_{1V}^\gamma = F_{1V}^Z = F_{1A}^Z = 1$ and all the others form factors are zero. The $t \to W^+b$ decay vertex can be treated in an analogous fashion. The form factors are typically corrected by a few percent or less from QCD and electroweak loops. Thus, any large deviations would indicate new physics.

Before beginning the analysis of the sensitivity of the NLC to these couplings, it is useful to re-emphasize the importance of polarization in the top quark interactions. In Fig. 3 I show the $t\bar{t}$ cross section as a function of the top quark production

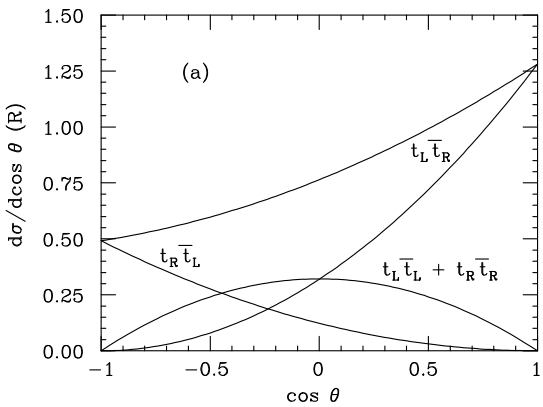

Fig. 3: $t\bar{t}$ cross section for left-polarized electrons.

angle for initial left-handed polarized electrons. By breaking down the event into helicity subprocesses, we see that much of the electron polarization is passed on to the top quarks. This spin transfer is perfect in the forward direction so that for large values of $\cos\theta$ we obtain a sample of highly polarized top quarks.

To make the most of this polarization, we must consider all of the helicity angles involved in the event. With Tim Barklow, I performed a tree-level study of the sensitivity to a maximum-likelihood analysis using all the information in the $t\bar{t}$ event[9]. The top mass was set to $m_t = 174$ GeV, and the the NLC parameters were chosen to be $\sqrt{s} = 400$ GeV, an integrated luminosity of 100 fb^{-1}, and 90% polarization for the electrons. Only the lepton+jets mode was included in the analysis, and a simple angular cut of $|\cos\theta_{\rm lab}| < 0.8$ was applied to all of the visible final-state particles.

In Fig. 4 I plot the 95% confidence level contours for F_{1V}^Z and F_{1A}^Z, obtained from

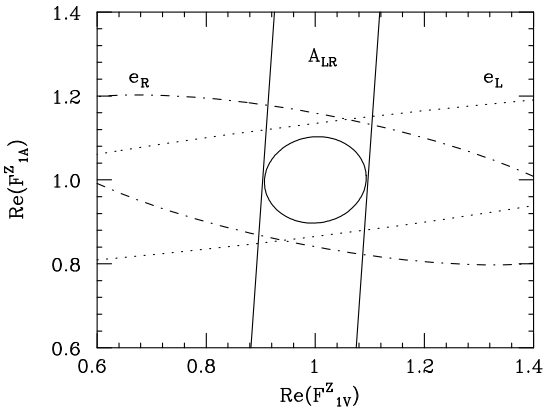

Fig. 4: 95% confidence level contours.

the maximum-likelihood analysis using a sample of 50 fb^{-1} each of right- and left-polarized electrons. This exhibits the degree to which we can probe the anomalous couplings of the top quark to the Z boson at the NLC. Note that the measurement of $A_{LR} = (\sigma_L - \sigma_R)/(\sigma_L + \sigma_R)$ is crucial for constraining the vector coupling to the Z boson. In fact, the use of polarized beams increases the sensitivity to this coupling by as much as a factor of 2. The combined 95% confidence level for the vector and axial-vector couplings yields an error of about 10% for this luminosity and these cuts. Surprisingly, the full maximum-likelihood analysis does not provide much extra sensitivity over an analysis based solely on the top quark production angle distribution—as long as the electron beam is polarized. A phenomenological analysis by Ladinsky and Yuan[10] of the production angle distribution of the top quark is consistent with these results.

In summary, there is much beautiful physics of the top quark to be explored at

the Next Linear Collider. In this talk I have only touched the surface.

References

[1] P. Zerwas, in *Physics and Experiments with Linear Colliders*, R. Orava, P. Eerola, and M. Nordberg, eds. (World Scientific, Singapore, 1992);
J. Kuhn, in *Physics and Experiments with Linear e^+e^- Colliders*, F. Harris, S. Olsen, S. Pakvasa, and X. Tata, eds. (World Scientific, Singapore, 1993).

[2] F. Abe *et al.* (CDF Collaboration), *Phys. Rev. Lett.* 74 (1995) 2626;
S. Abachi *et al.* (D0 Collaboration), *Phys. Rev. Lett.* 74 (1995) 2632.

[3] V. Fadin and V. Khoze, *JETP Lett.* **46** (1987) 525 and *Sov. J. Nucl. Phys.* **48** (1988) 309;
see also M. Strassler and M. Peskin, *Phys. Rev.* **D43** (1991) 1500.

[4] I would like to thank Michael Peskin for supplying me with Figs. 1(a) and (b).

[5] K. Fujii, T. Matsui, and Y. Sumino, *Phys. Rev.* **D50** (1994) 4341;
Y. Sumino, *Acta Phys. Polon.* **B25** (1994) 1837.

[6] M. Jezabek, J. Kuhn, and T. Teubner, *Z. Phys.* **C56**, (1992) 653;
M. Jezabek and T. Teubner, *Z. Phys.* **C59**, (1993) 669;
Y. Sumino, K. Fujii, K.Hagiwara, H. Murayama, and C.-K. Ng, *Phys. Rev.* **D47** (1993) 56.

[7] L.H. Orr, T. Stelzer, and W.J. Stirling, *Phys. Lett.* **B354** (1995) 442.

[8] C.R. Schmidt, preprint SCIPP-95/14 (1995), hep-ph-9504434.

[9] T.L. Barklow and C.R. Schmidt, in *DPF '94: The Albuquerque Meeting*, S. Seidel, ed. (World Scientific, Singapore, 1995).

[10] G.A. Ladinsky and C.-P. Yuan, *Phys. Rev.* **D49** (1994) 4415.